PERGAMON

Solid-State Electronics 46 (2002) 153–156

SOLID-STATE ELECTRONICS

Technical Note

Modeling inversion-layer carrier mobilities in all regions of MOSFET operation

K. Remashan, N.A. Wong, K. Chan, S.P. Sim, C.Y. Yang *

Microelectronics Laboratory, Santa Clara University, Santa Clara, CA 95053-0569, USA

Received 5 February 2001; received in revised form 21 August 2001

Abstract

Channel electron and hole mobilities in MOSFETs have been extracted in terms of the effective vertical field for several substrate biases. After ascertaining that the 2-D drift–diffusion numerical device simulator is reproducing the substrate charge variation in the MOSFET with respect to the gate voltage, obtained from C–V data, the mobility versus effective field behavior is extracted by comparing the simulated and measured I_d–V_{gs} characteristics. A simple model has been constructed to fit the extracted mobility data in weak and strong inversion, for inversion-layer electrons and holes in n-MOSFET and p-MOSFET, respectively. © 2002 Elsevier Science Ltd. All rights reserved.

Keywords: MOSFET; Mobility extraction; Modeling; Effective field; Drain current; Gate voltage

1. Introduction

The mobility of inversion-layer carriers is one of the key parameters underlying the MOSFET operation. The carrier mobility determines the drain current (I_d) drive, the transconductance (g_m), and the speed of the transistor, and is dependent on both the longitudinal (horizontal) and transverse (vertical) electric fields. RF circuits prefer to have MOSFETs operating in the moderate to weak inversion regions so that higher current efficiency (higher g_m/I_d) can be achieved [1]. Therefore, a need exists for a mobility model that can be used not only in the strong inversion region but also in the weak and moderate inversion regions. There are models which fit the mobility data in the low and high vertical field regions [2–5]. However, these models are complex and not suitable for incorporation into circuit simulators. This paper reports a simple model which accurately describes mobility in the low- and high-field regions and can be readily incorporated into existing circuit simulation programs.

In the next two sections, we present extraction of electron and hole mobilities versus effective vertical electric field and subsequent model development. A 2-D device simulator, MEDICI, which includes both the drift and diffusion components of the drain current (hence it works in weak and moderate inversion regions as well), is used to reproduce the extracted substrate charge. Moreover, the simulator takes into account Fermi–Dirac statistics and quantum mechanical effects, which are important in modern MOSFETs. Mobility values are then adjusted using MEDICI to fit the measured I_d–V_{gs} data. Two separate functions are used to fit the extracted mobility data for each carrier.

2. Electron mobility extraction and modeling

2.1. Electron mobility extraction

The mobility extraction technique used in our present work can be divided into two parts. First, the total semiconductor charge density (Q_S) calculated from the measured capacitance–voltage (C–V) behavior is compared with that obtained from MEDICI. Second, mobility is

* Corresponding author. Tel.: +1-408-554-6814; fax: +1-408-554-5474.

E-mail address: cyang@scu.edu (C.Y. Yang).

0038-1101/02/$ - see front matter © 2002 Elsevier Science Ltd. All rights reserved.
PII: S0038-1101(01)00285-4

extracted using MEDICI by comparing the simulated I_d–V_{gs} of the n-MOSFET with its measured counterpart. I–V data are then taken on MOSFETs with $W/L = 20$ μm/10 μm. Since the capacitance values of these devices are quite low and cannot be accurately determined using our LCR meter, we perform C–V measurements on large-area MOSFETs (269×1109 μm^2) from the same wafer. The extracted parameters from the C–V data are independent of device size.

The C–V measurement on a large-area n-MOSFET is taken between the gate and the substrate with the source and drain both connected to ground. Thus the measured capacitance reflects total charge variation in the semiconductor. The 10 kHz C–V curve for a 269×1109 μm^2 n-MOSFET is shown in the inset of Fig. 1. Oxide thickness is calculated from the maximum capacitance in the accumulation region. The doping concentration is estimated from the slope of the $1/C^2$ versus the gate voltage (V_g) curve in the depletion region. The flat-band voltage is then obtained from the extracted flat-band capacitance. The values of oxide thickness, doping concentration, and flat-band voltage obtained are 72.25 Å, 2.6283×10^{17} cm^{-3}, and -0.99 V, respectively.

The variation of Q_S with respect to V_g is obtained by integrating the 10 kHz C–V curve. This extracted charge is then compared with the simulated Q_S using MEDICI and the result is shown in Fig. 1. For computing Q_S with MEDICI, the parameters extracted from the C–V curve (oxide thickness, substrate doping, and flat-band voltage) are used. In addition, Fermi–Dirac statistics and quantum-mechanical effects are included in running MEDICI for optimal matching with Q_S from the C–V data. The quantum-mechanical model proposed by Van Dort et al. [6] is used in this simulation. The resulting match as shown in Fig. 1 is excellent.

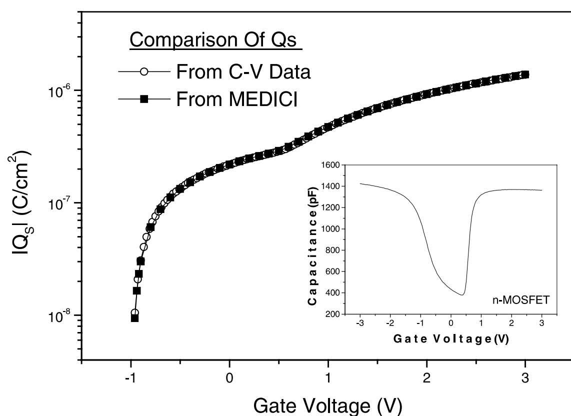

Fig. 1. Comparison of total semiconductor charge (Q_S) from the 10 kHz C–V data on n-MOSFET and that from MEDICI. Inset shows the 10 kHz C–V curve obtained between gate and substrate on a large-area n-MOSFET (source and drain both grounded, area $= 269 \times 1109$ μm^2).

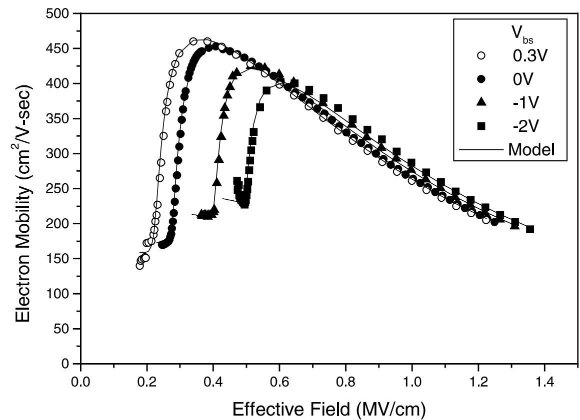

Fig. 2. Comparison of the extracted electron mobility data and the empirical model for substrate biases, 0.3, 0, −1, and −2 V. Measured I_d–V_{gs} characteristics for $V_{ds} = 40$ mV are used.

Having obtained the semiconductor charge, the only unknown parameter left which determines the drain current is the carrier mobility. Mobility is extracted from MEDICI by adjusting its values to fit the measured I_d–V_{gs} data for an n-MOSFET having $W/L = 20$ μm/10μm, with $V_{ds} = 40$ mV and $V_{bs} = 0.3, 0, -1$, and -2 V. Fig. 2 shows the mobility versus effective field behavior for $V_{bs} = 0.3, 0, -1$, and -2 V. The magnitude of the effective vertical field is calculated using $E_{eff} = (Q_i/2 + Q_b)/\epsilon_s$ [7,8], where Q_i is the inversion-layer charge density and Q_b is the depletion layer charge density. From Fig. 2, it is clear that mobility increases with E_{eff}, reaches a maximum, and then decreases. The mobility behavior in the higher electric field regime, which is known as the universal part, has been attributed mainly to phonon scattering and surface roughness scattering, while the mobility fall-off in the lower field region, the non-universal part, is due primarily to coulomb scattering from ionized impurities and other carriers [2,4]. It can be seen from Fig. 2 that in the lowest electric field region (weak inversion), the mobility is either leveling off or starting to bend upwards. In this region, the small channel carrier concentration probably results in enhanced mobility, as the scattering due to other carriers is minimal in the inversion layer.

We have extracted mobility data for two different drain voltages, namely, $V_{ds} = 40$ and 50 mV. There is no significant difference in the mobility data extracted between these two V_{ds} values, even for low E_{eff}. This is due to the fact that a long-channel device ($L = 10$ μm) is used for the extraction. For such a device, the lateral field is negligibly small even at $V_{ds} = 40$ mV, compared to E_{eff} in weak inversion. Thus the error introduced by the use of this V_{ds} value is expected to be insignificant.

2.2. Model generation for electron mobility

We now construct a simple empirical model to fit the mobility data. Two expressions are employed, one for the universal part, μ_{uni} [5], and the other for the non-universal part, $\mu_{non\text{-}uni}$ [9]. Using the Matthiessen-rule, the resulting fitted mobility is given by

$$\frac{1}{\mu} = \frac{1}{\mu_{uni}} + \frac{1}{\mu_{non\text{-}uni}} \tag{1}$$

where

$$\mu_{uni} = \frac{600\left(1 - \frac{V_{bs}}{29.5}\right)}{1 + \left(\frac{E_{eff}}{0.9}\right)^2}\ \mathrm{cm^2/V\,s} \tag{2}$$

and

$$\mu_{non\text{-}uni} = [250 - (100V_{bs})] + 300\left(\frac{N_i}{10^{11}}\right)\ \mathrm{cm^2/V\,s} \tag{3}$$

N_i is the electron concentration per unit area in the inversion layer. The mobility limit of 600 cm^2/V s in Eq. (2) is consistent with the bulk value for the extracted doping. The calculated mobilities for the substrate biases 0.3, 0, −1, and −2 V using Eqs. (1)–(3) are also shown in Fig. 2. It can be seen that the match between the extracted data and the empirical model is quite good. In our case, the extracted mobility shows a slight dependence of μ_{uni} on V_{bs}, which is not evident in Ref. [8]. We attribute this dependency to our assumption that the substrate doping is uniform.

3. Hole mobility extraction and modeling

3.1. Hole mobility extraction

The same procedure described in Section 2.1 is used here to extract the hole mobility. The 10 kHz C–V curve for a large-area p-MOSFET is shown in the inset of Fig. 3. The extracted doping concentration, oxide thickness, and flat-band voltage are 2.8128×10^{17} cm^{-3}, 72 Å, and 1.02 V, respectively. The total semiconductor charge density (Q_S) computed from the C–V curve and that from MEDICI are compared. The hole mobility is then obtained for substrate biases $V_{bs} = -0.3$, 0, 1, and 2 V. The extracted mobility versus the magnitude of the effective vertical field is shown in Fig. 4, where $E_{eff} = (Q_i/3 + Q_b)/\epsilon_s$ [8]. As in electron mobility, similar behavior is observed in the low-field regime, probably due to lessening of scattering from fewer holes present in the inversion layer.

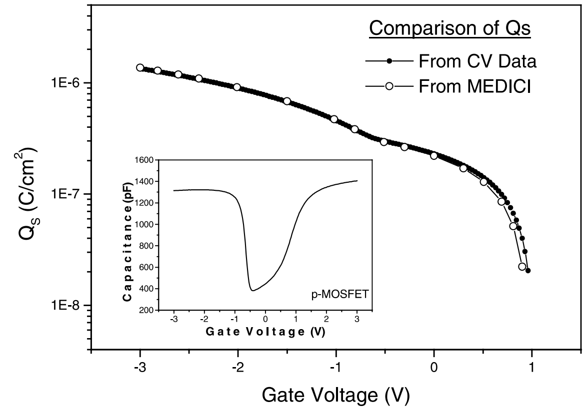

Fig. 3. Comparison of total semiconductor charge (Q_S) from the 10 kHz C–V data on p-MOSFET and that from MEDICI. Inset shows the 10 kHz C–V curve obtained between gate and substrate on a large-area p-MOSFET (source and drain both grounded, area = 269 × 1109 μm^2).

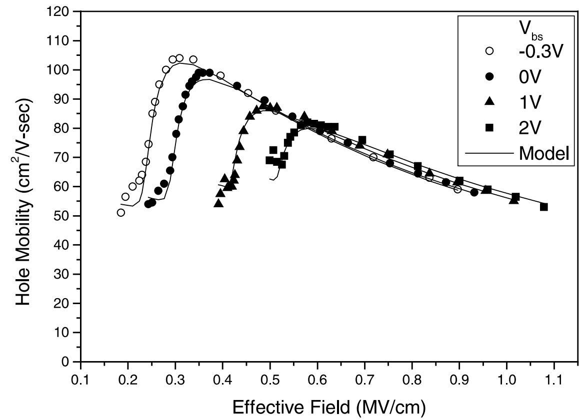

Fig. 4. Comparison of the extracted hole mobility data and the empirical model for substrate biases, −0.3, 0, 1, and 2 V. Measured I_d–V_{gs} characteristics for $V_{ds} = 40$ mV are used.

3.2. Model generation for the hole mobility

As in the previous section, two expressions, combined by the Matthiessen-rule given by Eq. (1), are used here to fit the extracted hole mobility data. The two expressions used are given below:

$$\mu_{uni} = \frac{192\left(1 + \frac{V_{bs}}{32}\right)}{1 + \left(\frac{E_{eff}}{0.45}\right)^{1.15}}\ \mathrm{cm^2/V\,s} \tag{4}$$

$$\mu_{non\text{-}uni} = [100 + (40V_{bs})] + 70\left(\frac{N_i}{10^{11}}\right)\ \mathrm{cm^2/V\,s} \tag{5}$$

N_i is the hole concentration per unit area in the inversion layer. As in electrons, Eq. (4) yields the correct bulk hole mobility value. The comparison between extracted mobilities and those calculated using the above model is given in Fig. 4. It can be seen that the match between the extracted data and the model is also reasonable.

The Eqs. (2)–(5) are simple closed-form representations of mobility for both electrons and holes in the low- and high-field regions, which can be incorporated into compact device models used in circuit simulators. Our model captures mobility data (from weak inversion to strong inversion) with two simple expressions as compared to complex expressions employed in Refs. [2,4]. Models given in those papers were intended primarily for device simulators. Also, the empirical formulas for μ_{uni} given by Eqs. (2) and (4) include both phonon and surface roughness scattering.

4. Conclusion

Inversion-layer mobility versus effective vertical electric field behavior has been examined for both electrons and holes with the help of a 2-D drift and diffusion device simulator, MEDICI, in conjunction with C–V and I–V characteristics of the MOSFETs. An empirical model for each carrier mobility versus effective field behavior is obtained, yielding reasonable fits to extracted data for all regions of MOSFET operation. The universal part of each carrier mobility model yields the correct bulk value, while the non-universal part shows some promise that coulomb scattering can be modeled accurately. Further investigation into substrate doping and substrate bias dependencies is in progress. In the low electric field or weak inversion regime, the anomalous behavior is attributed to reduction in carrier–carrier scattering in the inversion layer.

Acknowledgements

The authors gratefully acknowledge Professor K. Lee and Dr. N.D. Arora for their helpful advice and guidance.

References

[1] Enz C. RF MOS transistor modeling. 2000 FSA Design Modeling Work Shop. 2000. p. 1– 20.

[2] Villa S, Lacaita AL, Perron LM, Bez R. A physically-based model of the effective mobility in heavily-doped n-MOSFETs. IEEE Trans Electron Dev 1998;45:110–5.

[3] Mujtaba SA, Dutton RW, Scharfetter DL. Semi-empirical local NMOS mobility model for a 2-D device simulation incorporating screened minority impurity scattering. NUPAD V 1994:3–6.

[4] Shin S. Model for roll-off behaviour of electron effective mobility from universal curve. Electron Lett 1995;31:1789–91.

[5] Chen K, Wann HC, Ko PK, Hu C. The impact of device scaling and power supply change on CMOS gate performance. IEEE Electron Dev Lett 1996;17:202–4.

[6] Van Dort MJ, Woerlee PH, Walker J. A simple model for quantization effects in heavily-doped silicon MOSFETs at inversion conditions. Solid State Electron 1994;37: 411–4.

[7] Sun SC, Plummer JD. Electron mobility in inversion and accumulation layers on thermally oxidized silicon surface. IEEE Trans Electron Dev 1980;27:1497–508.

[8] Takagi S, Toriumi A, Iwase M, Tango H. On the universality of inversion layer mobility in Si MOSFETs: Part I. Effects of substrate doping concentration. IEEE Trans Electron Dev 1994;41:2357–68.

[9] Suetake M, Suematsu K, Nagakura H, Miura-Mattausch M, Mattausch HJ, Kumashiro S, Yamaguchi T, Odanaka S, Nakayama N. HiSIM: A drift–diffusion-based advanced MOSFET model for circuit simulation with easy parameter extraction. SISPAD 2000:261–4.